Trop J Nat Prod Res, April 2026; 10(4): 8628 – 8637

ISSN 2616-0684 (Print)
ISSN 2616-0692 (Electronic)

Tropical Journal of Natural Product Research

Available online at https://www.tjnpr.org

Original Research Article

Eco-Friendly Synthesis, Characterization, and Pharmacological Assessment of Silver Nanoparticles obtained from *Indigofera astragalina*: A Combined Approach to Antimicrobial and Antioxidant Therapeutics

Rajani Vallepu, and Umadevi Sankararajan*

School of Pharmaceutical Sciences, Vels Institute of Science, Technology & Advanced Studies (VISTAS), Pallavaram, Chennai, Tamil Nadu, India

ARTICLE INFO

Article history:
Received 21 February 2026
Revised 09 April 2026
Accepted 11 April 2026
Published online 01 May 2026

ABSTRACT

Nanotechnology and phytomedicine offer innovative methods for developing novel drugs. The ecologically friendly production of nanoparticles of silver (AgNPs) with substances derived from plants provides a biocompatible and environmentally acceptable substitute for traditional techniques by utilizing the inherent phytochemical bioactivity. *Indigofera astragalina* (IA), which is high in flavonoids and phenolic, was employed as a reductant and stabilizer. Silver nanoparticles produced with IA leaf extract (i.e. IA-AgNPs) were examined utilizing ultraviolet-visible light SEM/TEM, XRD, FTIR, and DLS. The results showed that the obtained IA-AgNPs were spherical, crystalline nanoparticles having an average size of 8.2 nm and excellent stability i.e. a zeta potential of -53.06 mV. The agar well diffusion method was used to assess its antimicrobial efficacy against species of Gram-positive (*S. aureus*, and *B. cereus*), Gram-negative (*E. coli*, and *K. pneumoniae*) and *Candida albicans* pathogens, followed by their MIC, MBC, and IC_{50} analysis. The MIC values of IA-AgNPs were 8–16 times lower than those of the crude extract, showing a marked higher level of dose-dependent inhibition. Significant efficacy was observed against *Candida albicans* (MIC: 0.78 µg/mL; IC_{50}: 0.6 µg/mL). IA-AgNPs demonstrated superior radical quenching ability, as evidenced by their antioxidant activity measured through superoxide scavenging assays (86.9%). The significant bio enhancement highlights a combined effect between the surface-bound phytochemicals and silver core, supporting the ethno pharmacological application of IA and establishing IA-AgNPs as a prospective multifunctional biotherapeutics that combat infections and scavenge free radicals.

Keywords: Green synthesis, Silver nanoparticles, *Indigofera astragalina*, Antimicrobial activity, Antioxidant activity.

Introduction

The continuing rise of antimicrobial resistance (AMR) is considered one of the most serious threats to global health in the twenty-first century. Many first-line therapies are becoming ineffective as pathogenic bacteria and fungi develop mechanisms to evade conventional antibiotics, which contributes to increased mortality, extended hospitalization, and greater healthcare costs.[1] Concurrently, Oxidative stress is defined as a condition in which the production of reactive oxygen species (ROS) exceeds the capacity of the body's antioxidant defenses, is implicated in several clinical conditions, including cancer, diabetes, cardiovascular disorders, and neurodegenerative conditions.[2] The dual burden of infectious and chronic degenerative diseases necessitates a continuous search for novel, safe, and effective therapeutic agents. Nanotechnology has emerged into a cutting-edge discipline offering innovative solutions owing to the unique physicochemical and biological properties of materials at the nanoscale (1–100 nm).[3]

*Corresponding author. E mail: umadevi.sps@vistas.ac.in
Tel: + 91 8667469884

Citation: Vallepu R, and Sankararajan U. Eco-Friendly Synthesis, Characterization, and Pharmacological Assessment of Silver Nanoparticles obtained from *Indigofera astragalina*: A Combined Approach to Antimicrobial and Antioxidant Therapeutics. Trop J Nat Prod Res. 2026; 10(4): 8628 – 8637 https://doi.org/10.26538/tjnpr/v10i4.45

Official Journal of Natural Product Research Group, Faculty of Pharmacy, University of Benin, Benin City, Nigeria

Among the wide range of nanomaterials, silver nanoparticles (AgNPs) have emerged as a subject of significant research interest because of their exceptionally broad-spectrum antibacterial activity, potent antioxidant properties, and comparatively low propensity to induce microbial resistance compared to traditional antibiotics.[4,5]The antimicrobial actions of AgNPs include adherence and instability of microbial cell membranes, cell penetration, oxidative stress generation through ROS formation, and disruption of vital cellular processes, including DNA replication and protein synthesis.[6,7]

Similarly, their antioxidant capacity is attributed to their ability to transport electrons or act as catalytic surfaces to neutralize free radicals, such as superoxide anions, hydroxyl radicals, and DPPH.[8] However, the conventional methods for generating AgNPs, such as chemical reduction, laser ablation, and thermal decomposition, often rely on hazardous reducing agents (such as sodium borohydride) and stabilizing chemicals (such as poly vinyl pyrrolidone), are energy-intensive, and result in environmentally hazardous byproducts.[9,10] These limitations raise significant concerns regarding the potential toxicity, environmental sustainability, and biocompatibility of the resultant nanoparticles for use in biomedical applications.

In accordance with the concepts of green synthesis chemistry, this has led to a paradigm shift in favor of "green synthesis" or biogenic synthesis. Green synthesis uses biological entities, such as bacteria, fungi, algae, and plant extracts, to reduce metal ions and stabilize the resultant nanoparticles.[11,12] Specifically, plant-mediated synthesis is the most widely used technique because of its vast range of phytochemicals, affordability, scalability, and ease of use. Plants contain secondary metabolites with inherent redox properties, including proteins, alkaloids, terpenoids, flavonoids, and phenolic acids.

Such compounds can effectively reduce metal ions (such as Ag^{+} to Ag^{0}.) and then cap the growing nanoparticles to prevent aggregation and offer

ISSN 2616-0684 (Print)
ISSN 2616-0692 (Electronic)

stability.[13] Crucially, these phytochemicals are not merely process facilitators but often possess intrinsic therapeutic properties. Plant-synthesized AgNPs are a synergistic hybrid system comprising a metallic nanoparticle core with robust bioactivity surrounded by a shell of bioactive phyto molecules that may provide novel or improved pharmacological effects.[14]

Therefore, selecting the appropriate plant species is essential. Traditional medicine systems in Asia and Africa have long employed several of the more than 700 species in the genus Indigofera (family Fabaceae). Many Indigofera species have been employed in the treatment of numerous illnesses, in particular epilepsy, gastrointestinal disorders, liver diseases, microbial infections, and inflammation.[15,16]*Indigofera astragalina* DC is an ethno medical plant commonly found in many regions of Africa and India. Traditional healers have used its leaves and roots to prepare pastes and decoctions for wounds, liver problems, cough, and diarrhea.[17] Preliminary scientific research has validated these applications.

Phyto chemical screening has revealed the abundance of alkaloids, phenolic acids, tannins, and flavonoids (including quercetin derivatives) in *I. astragalina*. Extracts from these plants have demonstrated strong antioxidant activity in several *in vitro* models due to their high phenolic and flavonoid content.[18-20] Furthermore, studies have demonstrated promising antibacterial activity against several bacterial and *fungal species*.[21] Recent studies have demonstrated significant inhibition of cell growth and *in vivo* antidiabetic properties, highlighting the therapeutic versatility of *I. astragalina* extract.[22,23]

Despite these encouraging results, the literature lacks a targeted and comparative investigation into the green synthesis of AgNPs using *I. astragalina* leaf extract, followed by a head-to-head assessment of the antimicrobial and antioxidant efficacy of the crude extract versus its nanoparticle derivatives. Therefore, it is essential to measure the "value addition" provided by nano technology in the food industry. Does the transformation of the extract into nanoparticles only maintain its bioactivity, or does it greatly increase it? The development of medicinal plant-based drugs will be significantly impacted by the answer to this question.

Therefore, the current study was designed with the following integrated goals in mind: (1) to perform a preliminary phytochemical profiling of the ethanolic leaf extract of *I. astragalina* (EEIA) to identify the bioactive constituents responsible for reduction and capping, (2) to optimize and carry out the green synthesis of silver nanoparticles (IA-AgNPs) using EEIA; (3) to thoroughly characterize the antimicrobial activity of the synthesized IA-AgNPs using *Gram-positive*, *Gram-negative*, and pathogenic fungi; and (4) to evaluate and compare their *in vitro* antioxidant potential using superoxide anion scavenging.

This study attempts to establish a preliminary scientific basis for the conventional use of *I. astragalina* while creatively investigating its potential in the emerging field of phyto-nanomedicine by fusing phytochemistry, nanotechnology, and pharmacology. The production of stable, bioactive IA-AgNPs using an environmentally friendly method may facilitate the synthesis of innovative, and sustainable bioactive nanomaterials against oxidative stress, infectious diseases and demonstrate their improved multifunctional capabilities

Materials and Methods

Chemicals and Reagents

Silver nitrate ($AgNO_3$, 99.9% purity) was purchased from Sigma-Aldrich (Germany). Mueller–Hinton agar (MHA), Sabouraud dextrose agar (SDA), and nutrient broth were obtained from HiMedia Laboratories Pvt. Ltd. (India). Standard antibiotic discs of ampicillin (10 µg), norfloxacin (10 µg), and Amphotericin B (20 µg) were sourced from HiMedia. For antioxidant assays, nitroblue tetrazolium (NBT), nicotinamide adenine dinucleotide (NADH), phenazine methosulfate (PMS), L-ascorbic acid, and Tris-HCl buffer were procured from Sigma-Aldrich. All other chemicals and solvents (ethanol, hydrochloric acid, ferric chloride, etc.) used for extraction and phytochemical testing were of analytical grade. Double-distilled water was used throughout the experiments to prepare the aqueous solutions.

Plant Material Collection and preparation of the extract

Indigofera astragalina was collected from local Mango fields (latitude 14.212482°, longitude 78.10958°), Kalasamudram, India, during the blossoming season (Fig.1). The plant was authenticated by Dr. K. Madhava Cheety, renowned taxonomist at the Department of Botany, Sri Venkateswara University, India. A voucher specimen with a voucher No. 0710 was kept at the Department of Botany, Sri Venkateswara University. The leaves were cleaned, placed on sterile blotting paper, and shade-dried at room temperature (25 ± 2°C) for approximately two weeks until their weight remained constant. The completely dried leaves were then pulverized into a fine powder using an electric grinder. To obtain the plant extract, 10 g of dried leaf powder was accurately weighed and subjected to extraction using a Soxhlet extraction apparatus. The extraction was performed with 100 mL of absolute ethanol as the solvent under continuous reflux at 80 °C for 30 minutes. This method is widely recognized for its efficiency in extracting both polar and moderately polar phytoconstituents. Following extraction, the extract was allowed to cool naturally to ambient temperature prior to further processing.[24]. Whatman No. 1 filter paper was used to filter out any remaining particles from the crude extract. The filtrate i.e. a concentrated ethanolic extract of *I. astragalina* (EEIA), was collected in a pre-weighed beaker. The solvent (i.e. ethanol) was removed at 40°C under reduced pressure using a rotary evaporator, to yield a semi-solid bulk mass. The extraction yield was calculated. The semi-solid EEIA was stored in an airtight, amber-colored glass jar at 4°C until needed. To prepare a stock solution for further research, the extract was reconstituted in ethanol or distilled water.

Figure 1: Morphological appearance of *Indigofera astragalina* collected for the present study.

Preliminary Phytochemical Screening of EEIA

Qualitative phytochemical analysis was performed on the EEIA using standard methods to identify the major classes of bioactive compounds present, namely alkaloids, phenolic compounds, tannins, flavonoids, and terpenoids.[25-27]

Green Synthesis of Silver Nanoparticles (IA-AgNPs)

IA-AgNPs were biosynthesized using a one-pot, redox-mediated method at high temperatures. A 1 mM aqueous solution was prepared by dissolving 0.0169 g of silver nitrate ($AgNO_3$) in 100 mL of double-distilled water. For the synthesis, 20 mL of the aqueous EEIA (obtained by dissolving the semi-solid extract in water to give a 10% w/v solution) was added drop wise while 80 mL of the 1 mM $AgNO_3$ solution was constantly magnetically agitated at 500 rpm. The mixture was then heated at a steady temperature of 70–80 °C on a hot plate. The reaction was allowed to continue for thirty to forty-five minutes.[28]

ISSN 2616-0684 (Print)
ISSN 2616-0692 (Electronic)

The reduction of Ag^+ ions to Ag^0 atoms and their subsequent nucleation and growth into nanoparticles were clearly observed by the color change of the reaction mixture from light yellowish-brown (the hue of the extract) to deep reddish-brown. This color shift is a well-known indicator that the Surface Plasmon Resonance (SPR) of silver nanoparticles is being stimulated.[29] A control setup with only the EEIA in water without $AgNO_3$ was maintained under the same conditions to confirm that the color shift was due to nanoparticle formation rather than extract degradation. Once the reaction was complete, the mixture was left to cool at room temperature. Centrifugation (Remi CPR-24 Plus) at 8000 rpm for 15 min was used to pellet the generated IA-AgNPs colloidal suspension. The supernatant, which was discarded, contained unreacted phytochemicals and silver ions. The pellet was rinsed three times with double-distilled water to remove any weakly attached biological molecules. To prevent hard agglomeration, it was re-dispersed using sonication (30 s) following each wash. The purified IA-AgNPs pellet was air-dried overnight in a sterile, dark environment to produce a fine powder. This powder was stored at 4°C in a sterile, light-proof container for subsequent characterization and bioactivity studies.

Characterization of Synthesized IA-AgNPs

UV-Visible Spectrophotometric Analysis

Ab initio, the AgNP synthesis was verified using a UV-Vis spectrophotometer (SL-159, ELICO Ltd., Hyderabad, India). The reaction mixture was collected at regular intervals, and its absorbance was scanned over the wavelength range of 300–700 nm using a quartz cuvette containing distilled water as the blank.[29,30] The maximum value of the characteristic SPR absorption peak (λmax) was recorded. The stability of the colloidal suspension was monitored by measuring the absorbance at λmax for seven days.

Fourier-Transform Infrared (FTIR) Spectroscopy

The functional groups of the phytochemicals responsible for the reduction of Ag^+ ions and capping/stabilization of the IA-AgNPs were identified using FTIR analysis. Hydraulic pressure was applied to compact the dry powder of EEIA and the biosynthesized IA-AgNPs into translucent pellets after mixing them in a 1:100 ratios with spectroscopic-grade potassium bromide (KBr). FTIR spectra were recorded using a PerkinElmer Spectrum Two spectrometer (PerkinElmer Inc., Waltham, MA, USA). In the transmittance mode between 400 and 4000 cm^{-1}, two spectrometers with a resolution of 4 cm^{-1} were employed.[31,32] The spectra were analyzed to identify characteristic peaks that matched specific bond vibrations (such as O-H, C=O, C-O-C, and N-H) and to document any changes or shifts in peak positions between the extract and nanoparticles that indicated interactions.

X-ray Diffraction (XRD) Analysis

The crystalline phase and structural characteristics of the IA-AgNPs were examined using X-ray diffraction (XRD). Dried nanoparticle powder was gently spread onto a clean glass slide for analysis. The XRD patterns were recorded using an X'Pert/PRO Analytical diffractometer (PANalytical B.V., Almelo, The Netherlands) equipped with Cu Kα radiation (λ = 1.5406 Å), operated at 40 kV and 30 mA. Data were collected over a 2θ range of 20°–80° with a step size of 0.02°. The obtained diffraction peaks were compared with the standard data available in the Joint Committee on Powder Diffraction Standards (JCPDS) database. The average crystallite size (D) of the IA-AgNPs was estimated from the most intense diffraction peak using the Debye–Scherrer equation (equation 1), where the full width at half maximum (FWHM) was taken into consideration.

$$D = \frac{(K\lambda)}{(\beta \cos\theta)} \qquad equation\ 1$$

Where: K is the Scherrer constant (shape factor, typically 0.9), λ is the X-ray wavelength, β is the FWHM in radians, and θ is the Bragg diffraction angle.[33]

Electron Microscopy and Elemental Analysis

SEM/TEM were employed to examine the surface morphology, size, and shape of the IA-AgNPs. For SEM analysis, a small amount of the IA-AgNP suspension was placed on a clean aluminum stub and allowed to dry at room temperature. To improve the conductivity, the sample was coated with gold using a sputter coater. Surface morphology was observed and captured using a JEOL JSM-IT200 scanning electron microscope operated at 15–20 kV.[34] TEM was used for size distribution analysis and high-resolution imaging. A drop of a very diluted IA-AgNPs suspension was placed on a copper grid coated with carbon and left to air dry. The prepared grid was analyzed using a JEOL JEM-2100 transmission electron microscope (JEOL Ltd., Tokyo, Japan) operated at an accelerating voltage of 200 kV. The particle size distribution was determined by measuring the diameters of at least 100 individual nanoparticles from the TEM micrographs using Image software (Version 1.53, National Institutes of Health, Bethesda, MD, USA).[35] We also used scanning electron microscopy (SEM) (JSM-6390, JEOL Ltd., Tokyo, Japan) coupled with energy-dispersive X-ray (EDX) spectroscopy (JSM-6390, JEOL Ltd., Tokyo, Japan) was employed to identify the elemental composition of the synthesized nanoparticles. The spectrum was captured multiple times to confirm the presence of elemental silver and other elements associated with the capping agents used in the synthesis

Dynamic Light Scattering (DLS) and Zeta Potential Analyses

The IA-AgNPs' hydrodynamic diameter (size distribution in solution) and surface charge (zeta potential) which are two crucial markers of colloidal stability, was examined with a Zetasizer Nano ZS (Malvern Instruments, UK). In an effort to prevent further dispersion effects, the IA-AgNPs colloidal suspension was appropriately diluted with double-distilled water before being placed in a disposable polystyrene cuvette for DLS. The observations were recorded under a scattering angle of 173 degrees especially at a temperature near twenty-five degrees Celsius. The intensity-weighted particle size distribution and polydispersity index (PDI) were displayed.[36] To determine the zeta potential, the same diluted material was placed inside a folded capillary cell. The electrophoretic mobility of the nanoparticles under an applied electric field was converted to zeta potential using Smoluchowski approximation. A highly negative or positive zeta potential (often > ±30 mV) indicates good electrostatic stability and low susceptibility to aggregation.[37]

Evaluation of Antimicrobial Activity

Microorganisms with Standard Culture

The antimicrobial potential of the samples were assessed against five clinically important human pathogens. The test organisms included the yeast *Candida albicans*, the antibacterial effect was tested on two types of *Gram-positive* bacteria, viz. *Staphylococcus aureus* (ATCC 29213) and *Bacillus cereus*, and two types of Gram-negative bacteria, i.e. *Escherichia coli* (ATCC 25922) and *Klebsiella pneumoniae* (ATCC 700603). The *C. albicans* and *B. cereus* strains were clinical isolates obtained from Cochin University. For inoculum preparation, bacterial strains were cultured overnight at 37 °C in Mueller–Hinton Broth (MHB), while the yeast culture was maintained at 30 °C in Sabouraud Dextrose Broth. The cultures in the exponential growth phase were adjusted with sterile saline to reach a turbidity equivalent to 0.5 McFarland standard which represents an approximate concentration of 1×10^8 CFU/mL for bacterial suspensions and 1×10^6 CFU/mL for the yeast.[38]

Agar Well Diffusion Assay

The antimicrobial activity was initially assessed by the agar well diffusion method. Briefly, 20–25 mL of Mueller–Hinton agar (MHA) for bacteria and Sabouraud dextrose agar (SDA) for *Candida albicans* were added to sterile Petri dishes, which were then allowed to solidify. A standardized microbial inoculum (100 µL) was uniformly swabbed onto the agar surfaces.

Wells of 10 mm diameter were made in the inoculated agar plates using a sterile cork borer. EEIA was evaluated at four concentrations (25, 50, 75, and 100 mg/mL). The extract was dissolved in distilled water supplemented with 1% DMSO to improve solubility. IA-AgNPs were

ISSN 2616-0684 (Print)
ISSN 2616-0692 (Electronic)

tested at 10 and 25 mg/mL in aqueous suspension, and a solvent control was included to rule out any effect of the vehicle. For each treatment group, 100 µL of the prepared solution was introduced into the corresponding well under aseptic conditions. To provide a benchmark for antimicrobial activity, commercially available antibiotic discs were used as positive controls viz. ampicillin (10 µg/disc), norfloxacin (10 µg/disc), and amphotericin B (20 µg/disc). After 30 min of pre-diffusion, the plates were incubated for 24–48 h at an appropriate temperature of 30°C for fungus and 37°C for bacteria. The inhibition zones were measured in millimeters. Each test was performed three times.[39,40]

After allowing the samples to diffuse for 30 minutes at room temperature, the inoculated plates were incubated for 24 to 48 hours. The fungal plates were maintained at 30 °C, while the bacterial plates were incubated at 37 °C. Upon completion of the incubation period, the zones of inhibition were carefully measured and recorded in millimeters. Each experiment was conducted in triplicate to confirm consistency of the results.

Determination of Minimum Inhibitory Concentration (MIC) and Minimum Bactericidal Concentration (MBC)

The MIC and MBC values were calculated using the broth microdilution method following the Clinical and Laboratory Standards Institute (CLSI) recommendations (M07-A11 and M27-A3). In sterile MHB (for bacteria) or Roswell Park Memorial Institute (RPMI-1640) medium buffered with 3-(N-morpholino) propane sulfonic acid (MOPS) (for *C. albicans*), two-fold serial dilutions of EEIA (0.78-100 µg/mL) and IA-AgNPs (0.097-12.5 µg/mL) were prepared in 96-well microtiter plates. A standardized microbial suspension (5×10^3 CFU/mL was added to each well. Plates were incubated for 24 h at 37°C for bacteria or for 48 h at 35°C for *Candida albicans*. The lowest concentration exhibiting no discernible turbidity was designated the minimum inhibitory concentration (MIC). Aliquots (10 µL) from the clear wells were sub cultured onto new agar plates to determine the MBC. Following incubation, the MBC was determined to be the lowest concentration that killed at least 99.9% of the original inoculum.[41]

Determination of IC_{50} for Antimicrobial Activity

The IC_{50} values represent the concentrations required to cause 50% inhibition of microbial growth and were determined using quantitative growth inhibition data from the broth micro dilution experiment. The optical density was measured at 600 nm using BioTek Synergy HTX Multi-Mode Microplate Reader (Agilent Technologies United States) after MIC determination to quantify the microbial growth in each well. Growth in the control wells was used to calculate the percentage of inhibition. IC_{50} values were calculated using non-linear regression analysis of the inhibition curves in GraphPad Prism software (version 9.0, Developed by GraphPad Software, United States)

Evaluation of Antioxidant Activity

Superoxide Anion ($O_2^{\bullet-}$) Scavenging

Superoxide radicals generated by the NADH/PMS system were identified by reducing nitroblue tetrazolium (NBT). The superoxide anion scavenging activity was tested using a non-enzymatic method adapted from Gutteridge *et al*.[42] Superoxide radicals were produced by a reaction mixture containing 1.5 mL of Tris-HCl buffer (32 mM, pH 8.0), 0.5 mL of NBT (0.3 mM), and 0.5 mL of NADH (0.468 mM). IA-AgNPs and EEIA were tested across a concentration range of 10–100 µg/mL. The reaction mixture consisted of Tris–HCl buffer (32 mM, pH 8.0), NBT (0.3 mM), NADH (0.468 mM), PMS (30 µM), was added 0.5 mL of the test samples (IA-AgNPs or EEIA; 10–100 µg/mL). The reaction was initiated by adding 1.0 mL PMS (Phenazine methosulfate) (30 µM). The mixture was vortexed and incubated at 25°C for five minutes. The intensity of the developed color was determined by measured at 560 nm using a UV–Visible spectrophotometer (SL-159, ELICO Ltd., Hyderabad, India) and compared to that of a blank (reaction mixture without PMS). Control reactions were performed without the test sample. Ascorbic acid was used as a standard reference antioxidant. The inhibition of superoxide anion was expressed as a percentage using equation 2

$$\%\ Inhibition = \left[\frac{(A_{control} - A_{sample})}{A_{control}}\right] \times \frac{100}{1} \qquad equation\ 2$$

Where: $A_{control}$ denotes absorbance of the control and A_{sample} is the absorbance in the presence of the test sample or standard.

Statistical Analysis

All antioxidant and antibacterial experiments were carried out in triplicate (n = 3). The results were reported as mean values with their corresponding standard deviations (mean ± SD). Statistical evaluation of the data was carried out using GraphPad Prism software version 9.0 (GraphPad Software Inc., San Diego, CA, USA). To compare the activity of EEIA and IA-AgNPs at different amounts, we used an unpaired Student's t-test. To compare multiple groups, like the tests for antioxidant effects at different doses, multiple group comparisons were evaluated using one-way ANOVA with Tukey's post-hoc analysis. Statistical significance was defined at a probability level of $p < 0.05$

Results and Discussion

Phytochemical Profiling of Indigofera astragalina Ethanolic Extract (EEIA)

Preliminary qualitative phytochemical analysis of the ethanolic leaf extract of *Indigofera astragalina* (EEIA) confirmed the presence of a broad spectrum of secondary metabolites in the extract. The extract tested positive for alkaloids, flavonoids, tannins, phenolic compounds, saponins, terpenoids, and proteins, whereas tests for reducing sugars were negative (Table 1). This profile is consistent with previous reports on the phytochemistry of *I. astragalina* and underscores the rich composition of bioactive compounds with inherent redox properties.[43]

Table 1: Phytochemicals of the ethanolic leaf extract (EEIA) from *I. astragalina*

Phytochemical Constituent	Test Name	Observation	Test
Alkaloids	Mayer's Test	Creamish-white precipitate formed	Present
Reducing sugars	Benedict's Test	No brick-red precipitate observed	Absent
Saponins	Foam Test	Persistent foam layer (>1 cm) formed	Present
Phenolic compounds	Ferric chloride test	Dark green coloration developed	Present
Tannins	Ferric chloride test	Brownish-green coloration observed	Present
Flavonoids	Ammonia test	Yellow color appeared and disappeared on standing	Present
Terpenoids			Present

The phytochemical profile of EEIA necessitated the synthesis of the nanoparticles.[44] Because of their hydroxyl and carbonyl groups, polyphenolic substances are good reducing agents that can donate electrons to change Ag^+ into Ag^0.[45] The FTIR spectrum changes and the remarkably high negative zeta potential (-53.06 mV) show that proteins and other macromolecules function as efficient capping agents, attaching to the developing nanoparticle surfaces to regulate development and prevent aggregation. Because the extract acts as a full

ISSN 2616-0684 (Print)
ISSN 2616-0692 (Electronic)

bioreactor and does not require external reducing and stabilizing chemicals, its dual function highlights the effectiveness of plant-mediated green synthesis.

Green Synthesis and Visual Observation of IA-AgNPs

To synthesize the silver nanoparticles (i.e. IA-AgNPs), light brown EEIA was mixed with a colorless 1 mM $AgNO_3$ solution at 70–80°C. The reduction of Ag^+ ions to Ag^0 [45]and the formation of nanoparticles were shown by the obvious and rapid color change from light brown to deep reddish-brown within 30 min (Fig. 2a). The role of the extract in promoting the redox process was demonstrated by the lack of color change in the control samples that contained only EEIA.

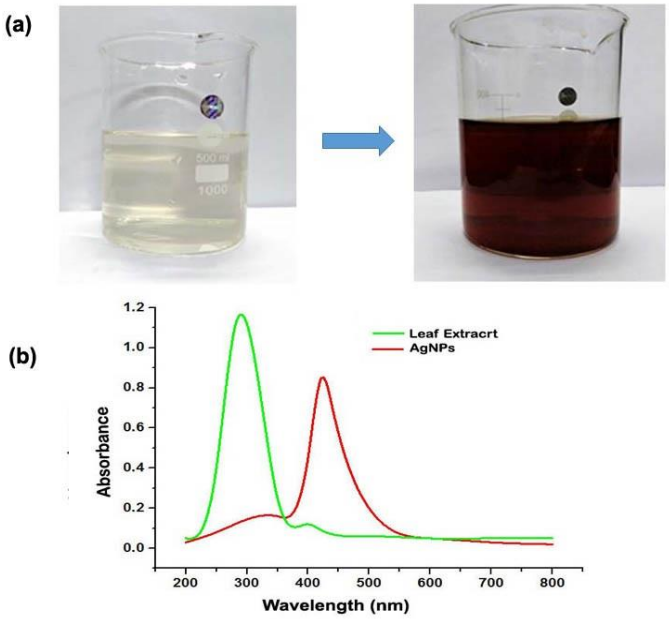

Figure 2: (a). Reaction mixture after 30 minutes showing deep reddish-brown color indicating nanoparticle formation, 2. (b). UV-Vis absorption spectrum of biosynthesized IA-AgNPs showing a characteristic Surface Plasmon Resonance peak at 422 nm.

UV-Visible Spectroscopic Characterization

UV-Vis spectral examination of the reaction mixture revealed a single, notable surface plasmon resonance (SPR) absorption peak centered at 422 nm (Fig. 2b).[46] The successful formation of IA-AgNPs was confirmed by this peak, which is characteristic of spherical Ag silver nanoparticles. The symmetry and sharpness of the peak indicate a relatively monodisperse population. The colloidal suspension did not considerably alter or widen the SPR peak for more than two weeks.

The characteristic SPR peak in UV-Vis spectroscopy at 422 nm confirmed the formation of spherical AgNPs. The peak's durability over time is consistent with the exceptional zeta potential value, which generates strong electrostatic repulsion between particles and guarantees colloidal stability an essential element for storage and biological applications. Similar results have been reported for plant-mediated AgNPs, where apple leaf extract showed an absorption maximum at 419 nm, and *Bauhinia variegata* mediated AgNPs exhibited a peak at 415 nm.[46, 47]

FTIR Spectroscopic Analysis

FTIR spectroscopy was applied to identify the chemical groups that were formed on the surface. This groups play essential role in stabilizing and capping of the nanoparticles, and the reduction reactions.[48] The EEIA spectra showed prominent bands for O–H stretching (~3375 cm^{-1}), C–H stretching (~2922, 2878 cm^{-1}), C=O stretching (~1611 cm^{-1}), and C–O stretching (~1053 cm^{-1}) (Fig. 3 a). In the IA-AgNPs spectrum (Fig. 3 b), these bands demonstrated notable shifts (e.g., O–H to ~3389 cm^{-1}, C=O to ~1602 cm^{-1}) and intensity variations, confirming the interaction of phenolic, carbonyl, and other oxygen-containing groups with the silver surface, promoting both reduction and stabilization of the AgNPs.[49]

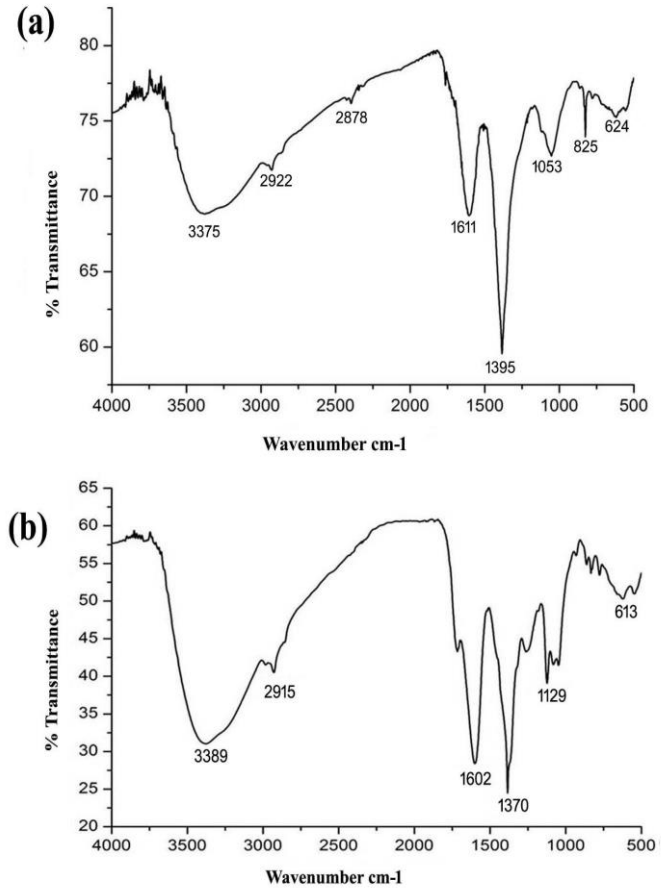

Figure 3: FTIR spectra of (a) ethanolic leaf extract of *I. astragalina* (EEIA) and (b) biosynthesized IA-AgNPs, showing shifts in characteristic peaks indicating the involvement of functional groups in reduction and capping

Crystallinity and Phase Analysis (XRD)

XRD analysis confirmed the crystallinity of the biosynthesized IA-AgNPs. Four distinct peaks in the diffraction pattern (Fig. 4 a) at 2θ values of 38.25°, 46.35°, 64.45°, and 76.83° reflected the (111), (200), (220), and (311) crystallographic planes of face-centered cubic (FCC) silver (JCPDS 04-0783). The strongest peak at (111) indicated the preferred crystal orientation. The average crystallite size was approximately 14 nm, according to the Debye-Scherrer equation from the (111) peak.[50, 51]

Morphological and Elemental Analysis

The SEM images (Fig. 4b)[52] show that IA-AgNPs were mostly spherical and widely distributed, with some aggregation caused by drying. Precise size and morphology information was obtained using higher-resolution TEM examination (Fig. 5a-b), which revealed spherical particles with an average diameter of 12 nm (range: 8–25 nm) based on the size distribution histogram (Fig. 5e). The XRD results were confirmed by the Selected Area Electron Diffraction (SAED) pattern (Fig. 4a), which displayed concentric rings corresponding to the FCC structure.[9,51] The elemental composition was verified by EDX spectroscopy (Fig. 4c), which revealed a significant signal for silver (Ag) at about 3 keV and weaker signals for carbon (C) and oxygen (O) from the phytochemical capping layer. [53]

ISSN 2616-0684 (Print)
ISSN 2616-0692 (Electronic)

XRD and SAED confirmed the crystalline FCC structure of the nanoparticles, which is characteristic of biogenic AgNPs and contributes to their designated physicochemical properties.[51] The small particle size (8–12 nm by TEM, 8.2 nm by DLS) is especially notable because it produces a high surface area-to-volume ratio, which is essential to the observed increased biological activity.

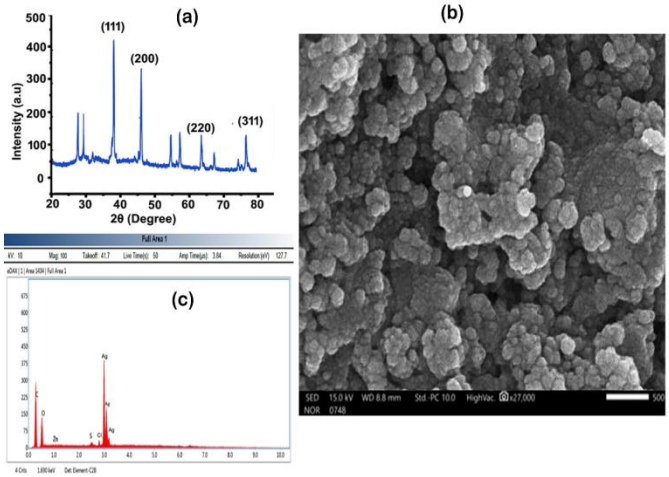

Figure 4: (a). X-ray diffraction pattern of IA-AgNPs, 4 (b). Representative SEM image of IA-AgNPs at 27,000× magnification (scale bar: 500 nm), showing agglomerated, roughly spherical nanoparticles. 4 (c). EDX spectrum showing a strong signal for silver (Ag) and signals for carbon (C) and oxygen (O) from the capping agents.

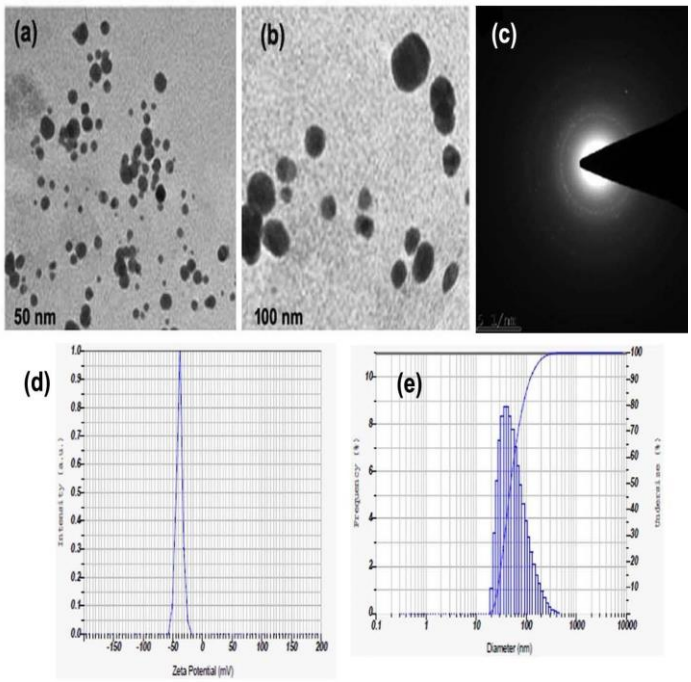

Figure 5: TEM analysis of spherical silver nanoparticles fabricated by IA leaf extract at magnification (a) 50 nm (b) 100 nm (c) SAED analysis (d) Zeta potential (e) Average particle size

Distribution of Particle Sizes and Colloidal Stability (DLS & Zeta Potential)

The IA-AgNPs revealed an intensity-weighted average hydrodynamics diameter of 20-80 nm and a polydispersity index (PDI) of 0.25, according to the DLS (dynamic light scattering) assay, confirming a comparatively monodisperse distribution (Fig. 5 e). Zeta potential test revealed a highly negative surface charge of -53.06 ± 2.1 mV (Fig. 5 d), indicating robust electrostatic stabilization and long-term colloidal stability. Bazmandeh *et al.*[54] reported that silver nanoparticles synthesized using *Stachys lavandulifolia* exhibited an average particle size of 164.8 nm with a zeta potential of −17.3 mV, indicating moderate stability of the nanoparticles.

Antimicrobial Activity

Both qualitative (agar well diffusion) and quantitative (MIC, MBC, IC_{50}) assays were used to systematically assess the antimicrobial efficacy of EEIA and IA-AgNPs against two Gram-positive bacteria (*Staphylococcus aureus* and *Bacillus cereus*), two Gram-negative bacteria (*Escherichia coli* and *Klebsiella pneumoniae*), and the pathogenic fungus i.e. *Candida albicans.*

Qualitative Assessment via Agar Well Diffusion

The Different inhibition zones demonstrated a concentration-dependent antibacterial activity of both EEIA and IA-AgNPs (Fig. 6). The crude extract (EEIA) showed moderate efficacy, with inhibitory zones ranging from 11 to 14 mm at 25 mg/mL and rising to 14–20 mm at the highest tested concentration (100 mg/mL).

However, IA-AgNPs demonstrated significantly greater antibacterial efficacy at much lower doses. Interestingly, 10 mg/mL IA-AgNPs produced inhibitory zones that were at least as broad as EEIA at 50–100 mg/mL in every organism examined. The most significant improvement was observed against *Candida albicans*, where IA-AgNPs at 10 and 25 mg/mL produced inhibition zones of 20 mm and 22 mm, respectively, significantly outperforming both EEIA at 100 mg/mL (14 mm) and the traditional antifungal Amphotericin B (10 mm).

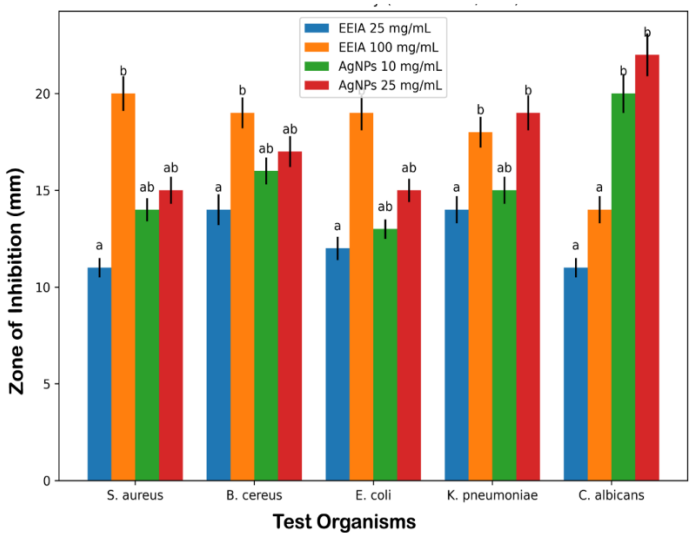

Figure 6: Comparative antimicrobial activity of *I. astragalina* ethanoic extract (EEIA) and IA-AgNPs against selected microbial strains. Values are presented as mean ± SD (n = 3). Different superscript letters (a–c) indicate statistically significant differences among groups ($p < 0.05$). IA-AgNPs exhibited significantly higher activity, particularly against *Candida albicans* ($p < 0.01$ compared to EEIA).

Quantitative Determination of MIC, MBC, and IC_{50} Values

The antibacterial potency was evaluated by determining MIC, MBC, and IC_{50} values using a standard broth microdilution assay tests to precisely evaluate the antimicrobial potency (Table 2). IA-AgNPs showed noticeably higher antibacterial activity, with MIC values 8–16 times lowers than those of the crude extract EEIA. IC_{50} values, derived from quantitative growth inhibition curves, provided additional evidence of the enhanced efficacy of the nano-formulation. *C. albicans*

ISSN 2616-0684 (Print)
ISSN 2616-0692 (Electronic)

had the lowest IC_{50} (0.6 ± 0.1 µg/mL) of all the species studied, with IA-AgNPs exhibiting IC_{50} values 10–20 times lower than the crude extract.

Table 2: Quantitative antimicrobial parameters of EEIA and IA-AgNPs against tested microorganisms

Microorganism	Sample	MIC (µg/mL)	MBC/MFC (µg/mL)	IC_{50} (µg/mL)
Staphylococcus aureus	EEIA	25.0	50.0	18.4 ± 1.2^a
	IA-AgNPs	3.12	6.25	2.1 ± 0.3^b
Bacillus cereus	EEIAF	12.5	25.0	9.8 ± 0.7^a
	IA-AgNPs	1.56	3.12	1.2 ± 0.2^b
Escherichia coli	EEIA	50.0	>100	35.6 ± 2.1^a
	IA-AgNPs	6.25	12.5	4.3 ± 0.5^b
Klebsiella pneumoniae	EEIA	25.0	50.0	17.9 ± 1.4^a
	IA-AgNPs	3.12	6.25	2.3 ± 0.4^b
Candida albicans	EEIA	12.5	25.0	8.9 ± 0.6^a
	IA-AgNPs	0.78	1.56	$\pm 0.1^b$

Note: Values are expressed as mean ± SD (n = 3). Different superscripts alphabets within the same microorganism indicate statistically significant differences ($p < 0.05$). EEIA – Ethanolic extract of *Indigofera astragalina* leaves. IA-AgNPs – Silver nanoparticles synthesized using EEIA.

The most obvious results of this work were the significant increases in antioxidant and antibacterial activities upon nano-formulation, which are now quantitatively supported by MIC, MBC, and IC_{50} data. The quantitative broth micro dilution experiments demonstrated a more significant improvement, but the crude EEIA demonstrated moderate, dose-dependent antibacterial action in the agar well diffusion assay. In comparison to the crude extract, IA-AgNPs showed 8–16 times lower MIC values and 10–20 times lower IC_{50} values. This enhanced effect may result from the combined action of different components acting on microbial cells.[53] More adherences to microbial membranes and improved cellular penetration are made possible by the nanoscale structure. The long-term release of Ag^+ ions by the nanoparticles can interfere with cellular respiration and energy consumption by binding to thiol groups in essential enzymes, such as respiratory chain enzymes.[55]

Additionally, AgNPs have the inherent ability to produce reactive oxygen species (ROS), which can oxidatively damage proteins, lipids, and DNA.[56] Also, an important advantage in the age of antimicrobial resistance is that the phytochemicals adds additional antimicrobial effects, such as membrane disruption by phenolics, resulting in a coordinated multi-target action that prevents the development of resistance.[57]

IC_{50} values, derived from quantitative growth inhibition curves, provided additional evidence of the enhanced efficacy of the nano-formulation. *C. albicans* had the lowest IC_{50} (0.6 ± 0.1 µg/mL) of all the species studied, with IA-AgNPs exhibiting IC_{50} values 10–20 times lower than the crude extract.

The considerably low MIC (0.78 µg/mL) and IC_{50} (0.6 µg/mL) values statistically validate the remarkable efficacy of the IA-AgNPs against *Candida albicans*. In the agar well diffusion assay, IA-AgNPs outperformed the conventional antifungal Amphotericin B by more than two times, and the quantitative results show that their potency was almost sixteen times higher than that of the crude extract. This points to a powerful, multimodal strategy against fungal cells that may involve direct interference with fungal DNA replication, rupture of the ergosterol-containing membrane, or strong interaction with the chitin and β-glucan cell wall.[58-60] For IA-AgNPs, the continuously close proximity of MBC to MIC values (usually a 2-fold difference) suggests a primarily bactericidal/fungicidal rather than bacteriostatic mode of action. This is especially helpful for clinical applications where pathogen eradication is crucial.

Antioxidant Activity
Superoxide Anion Scavenging Assay

Superoxide anion scavenging activity was concentration-dependent for both IA-AgNPs and EEIA (Fig. 7A). At dosages of 10–100 µg/mL, IA-AgNPs showed superior activity (~85% inhibition at 100 µg/mL) compared to EEIA (~78% inhibition). The standard, ascorbic acid, showed about 92% inhibition at the same concentration.

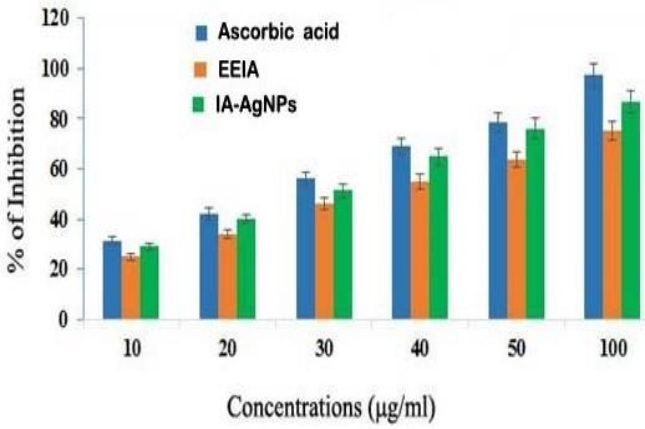

Figure 7: Antioxidant activity of EEIA and IA-AgNPs compared to ascorbic acid.

Correspondingly, the antioxidant capacity was significantly enhanced by the nanoparticle form. The superior superoxide scavenging capabilities of IA-AgNPs compared to the crude extract demonstrate that the nano-encapsulation process preserves and may even enhance the phytochemicals' redox activity. The nanoparticle matrix may protect antioxidant molecules from degradation, the silver core may have intrinsic catalytic (peroxidase-like) activity that aids in radical neutralization, or the large surface area may provide more active sites for radical interaction.[61,62]

The idea of "phyto-functionalized" nanoparticles is strongly supported by the convergence of these findings. According to this hypothesis, the green synthesis method produces bioactive hybrids in which the phytochemical shell and the metallic nanoparticle work in powerful concert rather than simply inert silver cores. By concentrating both Ag^+ ions and antimicrobial phytochemicals at the infection site and offering prolonged release kinetics, the nanoparticle serves as a targeted delivery platform for antimicrobial activity. The morphology maximizes the phytochemical's electron-donating efficiency for antioxidant activity while possibly enhancing the silver core's catalytic capabilities. This combination turns a conventional plant extract into a sophisticated

nanomaterial with several uses and greatly enhanced medicinal qualities.

The quantitative results provided here, particularly the low MIC, MBC, and IC_{50} values, place IA-AgNPs as a valid therapeutic candidate. The potency against *Candida albicans* (MIC: 0.78 µg/mL), which is equivalent to many conventional antifungals, is especially remarkable. Furthermore, its antibacterial activity against diverse bacterial groups, covering both Gram-positive and Gram-negative organisms gives credence to its potential for treating polymicrobial infections, and the antioxidant properties may help reduce oxidative tissue damage associated with infection.

Conclusion

The Phytochemistry of *Indigofera astragalina* is effectively utilized in the green synthesis of IA-AgNPs to produce stable, crystalline nanoparticles with remarkable bioactivity. Physicochemical analyses revealed predominantly spherical particles with a mean size of 8.2 nm and acceptable colloidal stability. *In vitro* comparisons indicated that IA-AgNPs displayed stronger antimicrobial and antioxidant effects than the crude extract, as reflected by its reduced MIC and IC_{50} values against the tested bacterial and fungal strains. This improvement in activity is most likely linked to the reduced particle size and the presence of plant-derived phyto constituents that remain associated with the nanoparticles. This study demonstrates the promising biological potential of *Indigofera astragalina*-derived silver nanoparticles. Although the findings indicate notable antimicrobial activity, further investigations are required to quantify silver content, evaluate Ag^+ release kinetics, clarify the mechanism of action, and establish a comprehensive safety profile. These additional studies will be essential to validate the therapeutic applicability of the synthesized nanoparticles and support their potential development for biomedical use.

Conflict of Interest

The authors declare no conflicts of interest.

Authors' Declaration

The authors hereby declare that the work presented in this article is original and that any liability for claims relating to the content of this article will be borne by them.

Acknowledgements

This study was supported by the School of Pharmaceutical Sciences addressed to Dr. S. Umadevi, Associate Professor, School of Pharmaceutical Sciences, Vels Institute of Science, Technology & Advanced Studies (VISTAS), Pallavaram, Chennai, Tamil Nadu, India.(Remove) The authors are thankful to Dr. C. Naga Raju, Assistant Professor, Department of Biochemistry, Sri Vani Degree and PG College, Ananthapuramu, Andhra Pradesh, India for extending his help in proof reading of the Manuscript.

References

1. More PR, Pandit S, Filippis AD, Franci G, Mijakovic I, Galdiero M. Silver nanoparticles: bactericidal and mechanistic approach against drug resistant pathogens. Microorganisms. 2023; 11(2):369.
2. Jeevan Kumar SP, Rajendra Prasad S, Banerjee R, Thammineni C. Seed birth to death: dual functions of reactive oxygen species in seed physiology. Ann Bot. 2015; 116(4):663-668.
3. Meher A, Tandi A, Moharana S, Chakroborty S, Mohapatra SS, Mondal A, Dey S, Chandra P. Silver nanoparticle for biomedical applications: a review. Hybrid Adv. 2024; 6:100184.
4. Bruna T, Maldonado-Bravo F, Jara P, Caro N. Silver nanoparticles and their antibacterial applications. Int. J Mol. Sci. 2021; 22(13):7202.
5. Wahab S, Khan T, Adil M, Khan A. Mechanistic aspects of plant-based silver nanoparticles against multidrug-resistant bacteria. Heliyon. 2021; 7(7): e07448.
6. Jiang X, Khan S, Dykes A, Stulz E, Zhang X. Biogenic synthesis of silver nanoparticles and their diverse biomedical applications. Molecules. 2025; 30(15):3104.
7. Nasrollahi A, Pourshamsian KH, Mansourkiaee P. Antifungal activity of silver nanoparticles on some fungi. Int. J Nano Dimens. 2011; 1(3):233-239.
8. Netala VR, Bukke S, Domdi L, Soneya S, Reddy SG, Bethu MS, Kotakdi VS, Saritha KV, Tartte V. Biogenesis of silver nanoparticles using leaf extract of *Indigofera hirsuta* L. and their potential biomedical applications (3-in-1 system). Artif Cells Nanomed Biotechnol. 2018; 46(Suppl 1):1138-1148.
9. Song JY, Kim BS. Rapid biological synthesis of silver nanoparticles using plant leaf extracts. Bioprocess Biosyst Eng. 2009; 32(1):79-84.
10. Fahim M, Shahzaib A, Nishat N, Jahan A, Bhat TA, Inam A. Green synthesis of silver nanoparticles: a comprehensive review of methods, influencing factors, and applications. J Colloid Interface Sci. Open. 2024; 16:100125.
11. Vanlalveni C, Lallianrawna S, Biswas A, Selvaraj M, Changmai B, Rokhum SL. Green synthesis of silver nanoparticles using plant extracts and their antimicrobial activities: a review of recent literature. RSC Adv. 2021; 11(5):2804-2837.
12. Chopra H, Bibi S, Singh I, Hasan MM, Khan MS, Yousafi Q, Baig AA, Rahman MM, Islam F, Emran TB, Cavalu S. Green metallic nanoparticles: biosynthesis to applications. Front Bioeng Biotechnol. 2022; 10:874742.
13. Hosny S, Gaber GA, Ragab MS, Ragheb MA, Anter M, Mohamed LZ. A comprehensive review of silver nanoparticles (AgNPs): synthesis strategies, toxicity concerns, biomedical applications, AI-driven advancements, challenges, and future perspectives. Arab J Sci. Eng. 2025.
14. Das S, Das J, Samadder A, Bhattacharyya SS, Das D, Khuda-Bukhsh AR. Biosynthesized silver nanoparticles by ethanolic extracts of *Phytolaccadecandra*,*Gelsemiumsempervirens*, *Hydrastiscanadensis* and *Thujaoccidentalis* induce differential cytotoxicity through G2/M arrest in A375 cells. Colloids Surf B Biointerfaces. 2013; 101:325-336.
15. Gerometta E, Grondin I, Smadja J, Frederich M, Gauvin-Bialecki A. A review of traditional uses, phytochemistry and pharmacology of the genus Indigofera. J Ethnopharmacol. 2020; 253:112608.
16. Rajani V, Umadevi S, Naga Raju C. A review on exploring the phytochemical and pharmacological significance of *Indigofera astragalina.* Pharmacogn Mag. 2024; 20(2):363-371.
17. Manivannan R, Shiju VM, Senthil KR. Radical scavenging and antioxidant activities of successive solvent extracts of *Indigofera astragalina*. Isr J Plant Sci. 2016; 64(1-2):33-43.
18. Abdoulahi MI, Sahabi B, Abdelkader AS, Tidjani IA, Chaïbou Y, Chaibou M, Laouali AI, Martin K, Hassimi S. Phytochemical investigation and antimicrobial activity of six plants used in children's ailments treatment in Niger. J Dis Med Plants. 2020; 6(4):92-97.
19. Madhavi B, Arigari NK, Srinivas KV, Kumar JK, Ravi G, Mohan GK. In vitro antioxidant activity profiling of *Indigofera astragalina* DC extracts along with estimation of total phenolic and flavonoid content. Int. J Pharm Biol. Sci. 2018; 8(4):1071-1076.
20. Gafar MK, Itodo AU, Atiku FA, Hassan AM, Peni IJ. Proximate and mineral composition of the leaves of hairy indigo *(Indigofera astragalina*). Pak J Nutr. 2011; 10(2):168-175.
21. Bello OM, Zaki AA, Khan SI, Fasinu PS, Ali Z, Khan IA, Usman LA, Oguntoye OS. Assessment of selected medicinal plants indigenous to West Africa for anti-protozoal activity. South Afr. J Bot. 2017; 113:200-211.

22. Manoharan S, Kanagavalli R, Raju SK, Rangasamy M. Phytochemical analysis and in vitro cytotoxic activity of various extracts of *Indigofera astragalina*. Pharm Lett. 2015; 7:206-210.
23. Shirsat MK, Mathew SV. Phytochemical and anti-diabetic activity of Indigofera species. J Drug Deliv. Ther. 2019; 9(4-s):1054-1059.
24. Do QD, Angkawijaya AE, Tran-Nguyen PL, Huynh LH, Soetaredjo FE, Ismadji S, Ju YH. Effect of extraction solvent on total phenol content, total flavonoid content, and antioxidant activity of *Limnophila aromatica*. J Food Drug Anal. 2014;22(3):296–302.
25. Onochie AU, Oli AH, Oli AN, Ezeigwe OC, Nwaka AC, Okani CO, Okam PC, Ihekwereme CP, Okoyeh JN. The pharmacobiochemical effects of ethanol extract of *Justicia secunda*Vahl leaves in *Rattus norvegicus*. J Exp. Pharmacol. 2020; 12:423-437.
26. Zulcafli AS, Lim C, Ling AP, Chye S, Koh R. Focus: plant-based medicine and pharmacology: Antidiabetic potential of Syzygium sp.: an overview. Yale J Biol. Med. 2020; 93(2):307-325.
27. Godlewska K, Pacyga P, Najda A, Michalak I. Investigation of chemical constituents and antioxidant activity of biologically active plant-derived natural products. Molecules. 2023; 28(14):5572.
28. Sivalingam AM, Pandian A. Identification and characterization of silver nanoparticles from *Erythrina indica* and its antioxidant and uropathogenic antimicrobial properties. Microb Pathog. 2024; 190:106635.
29. HabeebRahuman HB, Dhandapani R, Narayanan S, Palanivel V, Paramasivam R, Subbarayalu R, Thangavelu S, Muthupandian S. Medicinal plants mediated green synthesis of silver nanoparticles and their biomedical applications. IET Nanobiotechnol. 2022; 16(4):115-144.
30. Miškovská A, Michailidu J, Kolouchová IJ, Barone L, Gornati R, Montali A, Tettamanti G, Berini F, Marinelli F, Masák J, Čejková A. Biological activity of silver nanoparticles synthesized using viticultural waste. Microb Pathog. 2024; 190:106613.
31. Yassin MT, Mostafa AA, Al-Askar AA, Al-Otibi FO. Facile green synthesis of silver nanoparticles using aqueous leaf extract of *Origanum majorana* with potential bioactivity against multidrug-resistant bacterial strains. Crystals. 2022; 12(5):603.
32. Madakka M, Jayaraju N, Rajesh N. Evaluating antimicrobial and antitumor screening of green synthesized silver nanoparticles using *Syzygium jambolanum* against MCF-7 breast cancer cell line. J Photochem Photobiol. 2021; 6:100028.
33. Zia F, Ghafoor N, Iqbal M, Mehboob S. Green synthesis and characterization of silver nanoparticles using *Cydonia oblonga* seed extract. Appl. Nanosci. 2016; 6:1023-1029.
34. Palanivel C, Prabhakaran NR, Selvakumar G. Morphological expedient flower-like nanostructures WO_3–TiO_2 nanocomposite material and its multi applications. Open Nano. 2019; 4:100026.
35. Jaast S, Grewal A. Green synthesis of silver nanoparticles, characterization and evaluation of their photocatalytic dye degradation activity. Curr Res Green Sustain Chem. 2021; 4:100195.
36. Wei S, Wang Y, Tang Z, Xu H, Wang Z, Yang T, Zou T. A novel green synthesis of silver nanoparticles by the residues methylene blue dye and Hg^{2+} biosensing. SN Appl Sci. 2020; 2(4):1–16.
51. Awwad AM, Salem NM, Abdeen AO. Green synthesis of silver nanoparticles using *carob* leaf extract and its antibacterial activity. Int. J Ind. Chem. 2013; 4(1):29.
52. Choi JS, Lee JW, Shin UC, Lee MW, Kim DJ, Kim SW. Inhibitory activity of silver nanoparticles synthesized using *Lycopersicon esculentum* against biofilm formation in Candida species. Nanomaterials. 2019; 9(11):1512.

of Chinese herbal medicine and their biological activities. RSC Adv. 2021; 11(3):1411-1419.
37. Hosokawa M, Nogi K, Naito M, Yokoyama T. Nanoparticle Technology Handbook. (2nd ed.) Amsterdam: Elsevier; 2007.
38. Rajeshkumar S, Rinitha G. Nanostructural characterization of antimicrobial and antioxidant copper nanoparticles synthesized using novel *Persea americana* seeds. Open Nano. 2018; 3:18-27.
39. El-Adawy MM, Eissa AE, Shaalan M, Ahmed AA, Younis NA, Ismail MM, Abdelsalam M. Green synthesis and physical properties of Gum Arabic-silver nanoparticles and its antibacterial efficacy against fish bacterial pathogens. Aquac Res. 2021; 52(3):1247-1254.
40. Kumar VM, Thippeswamy B, Shivakumar C. Evaluation of antimicrobial activity of Bacillus cereus and Bacillus pumillus metabolites against human pathogens. Int. J Curr. Pharm Rev Res. 2013; 4(2):47-60.
41. Collee JG, Fraser AG, Marmion BP, Simmons A. Mackie and McCartney practical medical microbiology. (14th ed.) New York: Churchill Livingstone; 1996.
42. Raju CN, Rajani V, Anuradha CM, Kumar CS, Ramana PV, Sanjeeva P, Subbarao B, Mallaiah P, Reddy PR, Rao KY. Experimental and computational studies of novel amide analogues of ferulic acid as potential MDM2 inhibitors to retrieve p53 function. J Mol. Struct. 2024;1313:138635.
43. Mohammed BS, Sutramay P, Ahmadi S, Fathima S, Askani S, Jambiga PC, Thumma R, Dharavath SB, Taduri S. Phytochemical screening and anti-bacterial activity of *Erythrina variegata* leaf, stem and root extracts. J Plant Dev. 2023; 30:77-87
44. Nilavukkarasi M, Vijayakumar S, Kumar SP. Biological synthesis and characterization of silver nanoparticles with *Capparis zeylanica* L. leaf extract for potent antimicrobial and antiproliferative efficiency. Mater Sci Energy Technol. 2020; 3:371–376
45. 376REMOVE Simić A, Manojlović D, Šegan D, Todorović M. Electrochemical behavior and antioxidant and prooxidant activity of natural phenolics. Molecules. 2007; 12(10):2327-2340.
46. Kazlagić A, Abud OA, Ćibo M, Hamidović S, Borovac B, Omanović-Mikličanin E. Green synthesis of silver nanoparticles using apple extract and its antimicrobial properties. Health Technol. 2020; 10(1):147-150.
47. Soliman MK, Hashem AH, Al-Askar AA, AbdElgayed G, Salem SS. Green synthesis of silver nanoparticles from *Bauhinia variegate* and their biological applications. Green Process Synth. 2024; 13(1):20240099
48. Hiral V, Rahul S, Shailesh V, Amanullakhan P. Biosynthesized silver nanoparticles using an aqueous root extract of *Iris germanica* as a reducing agent and its antibacterial efficacy. Eur J Med Plants. 2020; 31(10):1-10.
49. Pourmortazavi SM, Taghdiri M, Makari V, Rahimi-Nasrabadi M. Procedure optimization for green synthesis of silver nanoparticles by aqueous extract of *Eucalyptus oleosa*. *SpectrochimActa* A: Mol Biomol Spectrosc. 2015; 136:1249–1254.
50. Kadam J, Dhawal P, Barve S, Kakodkar S. Green synthesis of silver nanoparticles using cauliflower waste and their multifaceted applications in photocatalytic degradation of
53. Ahmed S, Ahmad M, Swami BL, Ikram S. A review on plants extract mediated synthesis of silver nanoparticles for antimicrobial applications: a green expertise. J Adv. Res. 2016; 7(1):17-28.
54. Bazmandeh AZ, Rezaei A, Jafarbigloo HRG, Javar AMA, Hassanzadeh A, Amirian A, Mehrabi M. Green synthesis and characterization of biocompatible silver nanoparticles using *Stachys lavandulifolia* Vahl extract and their antimicrobial

performance study. J Environ Treat Tech. 2020; 8(1):284-290
55. Vidyasagar, Patel RR, Singh SK, Singh M. Green synthesis of silver nanoparticles: methods, biological applications, delivery and toxicity. Mater Adv. 2023; 4:1831–1849.
56. Sati A, Ranade TN, Mali SN, Yasin HKA, Pratap A. Silver nanoparticles (AgNPs): comprehensive insights into bio/synthesis, key influencing factors, multifaceted applications, and toxicity—a 2024 update. ACS Omega. 2025; 10(8):7549–7582
57. Dogiparthi LK, Sana SS, Shaik SZ, Kalvapalli MR, Kurupati G, Kumar GS, Gangadhar L. Phytochemical mediated synthesis of silver nanoparticles and their antibacterial activity. SN Appl. Sci. 2021; 3(6):631.
58. El-Saadony MT, Saad AM, Mohammed DM, Korma SA, Alshahrani MY, Ahmed AE, Ibrahim EH, Salem HM, Alkafaas SS, Saif AM, Elkafas SS. Medicinal plants: bioactive compounds, biological activities, combating multidrug-resistant microorganisms, and human health benefits—a comprehensive review. Front Immunol. 2025; 16:1491777.
59. Sidhu AK, Verma N, Kaushal P. Role of biogenic capping agents in the synthesis of metallic nanoparticles and evaluation of their therapeutic potential. Front Nanotechnol. 2022; 3:801620.
60. Feng QL, Wu J, Chen GQ, Cui FZ, Kim TN, Kim JO. A mechanistic study of the antibacterial effect of silver ions on *Escherichia coli* and *Staphylococcus aureus.* J Biomed Mater Res. 2000; 52(4):662–668.
61. Khuda F, Gul M, Ali Khan Khalil A, Ali S, Ullah N, Shafiq Khan M, Nazir S, Irum Khan S, Mehtap Büyüker S, Almawash S, Shafique M, Shah SA. Biosynthesized silver Nanoparticles using *Alnus nitida* Leaf Extract as a Potential Antioxidant and Anticancer Agent. ACS Omega. 2023; 8(33):30221-30230.
62. Ullah S, Khalid R, Rehman MF, Irfan MI, Abbas A, Alhoshani A, Anwar F, Amin HMA. Biosynthesis of phyto-functionalized silver nanoparticles using olive fruit extract and evaluation of their antibacterial and antioxidant properties. Front Chem. 2023; 11:1202252.